ATCA Upgrade - Pointing considerations

M.Kesteven

March 23, 1998

AT document 39.3/081

1 The Problems

Operation of the Compact Array at 3mm will impose some serious conditions on the tracking ability of the antennas; studies by Holdaway and others (Holdaway, 1997; Butler, 1997) indicate that the requirements should be :

Table 1: Pointing requirements

mapping mode	pointing rms	80 GHz pointing rms
single pointing	< beamwidth / 10.	4.2 asec
mosaicing	< beamwidth / 30.	1.6 asec

This note outlines some of the technical hurdles that need to be overcome :

1. Wind load deformations.
2. Servo loop issues.
3. Thermal deformations.
4. Accuracy of the pointing model.
5. Anomalous (and nomalous) refraction.

2 Wind Loading

Operation in windy conditions is likely to be difficult, in at least two aspects:

(a) The wind load on the reflector surface will deform the backup structure.

(b) The load may also result in a pointing shift if the wind-induced torques are not fully countered by the servo loop. This matter is discussed in section 3.

Table 2: Wind Loading Summary

θ (degrees)	full path rms (mm)	pointing shift (arcsec)	corrected path rms (mm)
0	0.19	3	0.16
60	0.65	-13	0.34
90	0.64	23	0.06
120	0.77	-28	0.11
180	0.12	1	0.12

θ is the angle between the optical axis and the wind vector

Connell-Wagner (J. Schafer) have carried out a series of computations on the deformations expected for a wind speed of 8 m/s (29 km/hr), for a number of antenna-wind orientions. The results are summarised in Table 2. The calculations used the JPL wind-tunnel data for a solid paraboloid with F/D of 0.33 (Fox et al, 1962). This data parallels the work done for the AT in 1983 (Melbourne et al). (The AT study used porous panels over the entire surface).

The JPL study was of a paraboloid in isolation, and therefore ignores the shadowing effect of the pedestal structure, as well as any shadowing due to the backup structure.

Figure 1 shows the results of the calculations for the worst case: with the wind vector at 60 degrees to the radio axis.

The calculations show that mm operations will be difficult in windy conditions.

The weather data at narrabri has been examined in some detail - 10 second snapshots have been recorded for the past few years. One summary is shown in figure 2. This shows the day/night median wind speeds recorded each month. During the mm season (may-november), at night, the median is below 1 m/sec. Since the wind load is proportional to the square of the wind speed, we conclude that the median deformations of table 2 will be reduced by a factor of ~ 64, bringing them into a tolerable range.

Figure 3 provides a different view of the data - it shows, for each month since 1996, the fraction of the time for which the wind contribution to the pointing error was less than 1 arcsecond.

conclusion #1 : night-time observations will in general not be compromised by wind-induced effects.

The sample-to-sample stability of the wind data has also been examined. Even in the higher wind speed conditions the changes from sample to sample are small - < 2 m/s (magnitude) and < 4 degrees (direction); this suggests that a pointing correction for the wind is possible. This could be done in several ways:

(a) reference pointing would, in principle, correct for the mean wind speed and direction.

(b) one could imagine a link between the antenna servo loop and an anemometer, along with a calibration table.

conclusion #2 : some relief in windy conditions is possible.

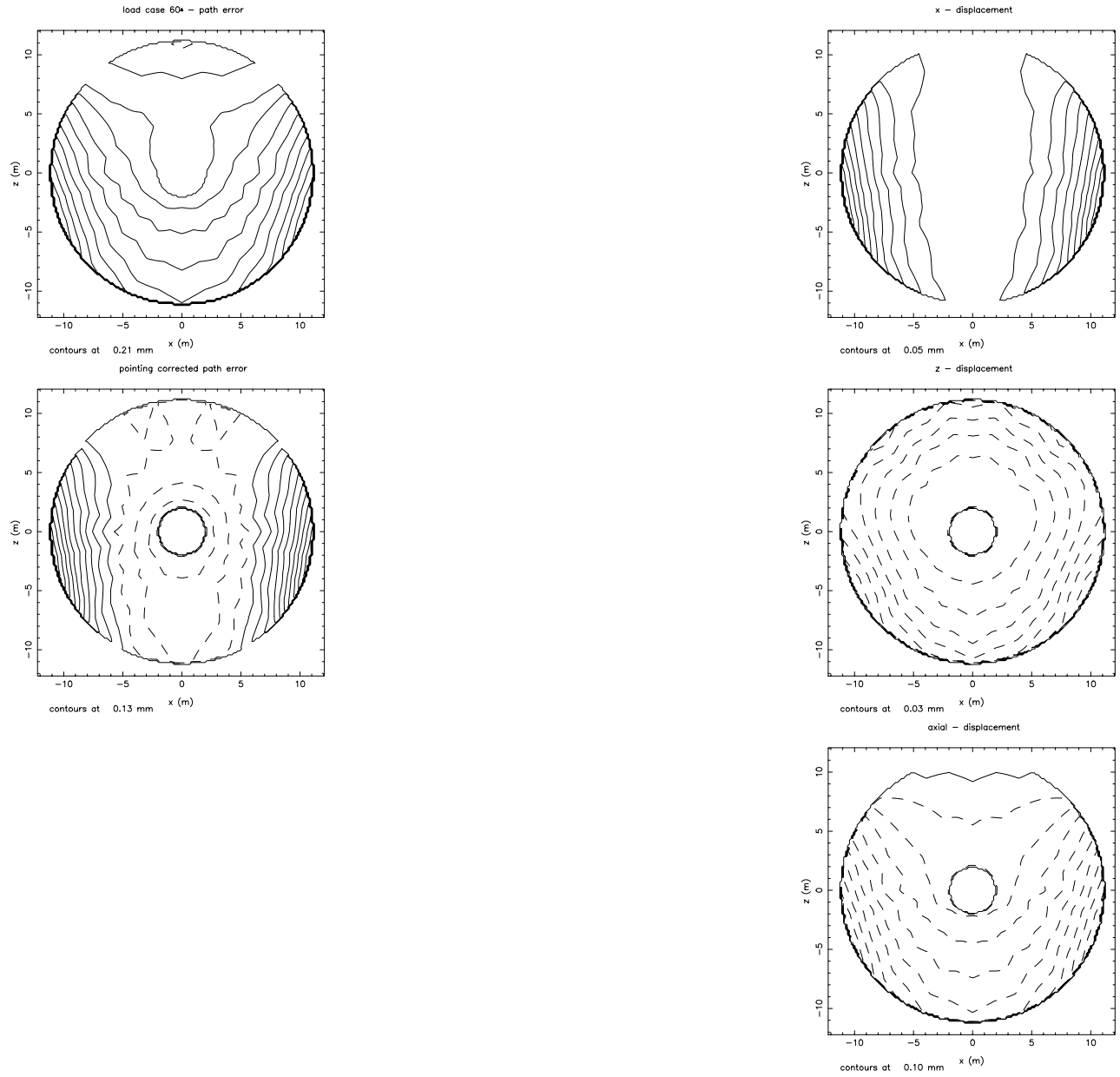

Figure 1: The antenna deformations for a wind speed of 8 m/s, incident at 60 degrees to the radio axis. This is the angle with the greatest deformation. The left hand column shows the effect of the deformations: the phase distribution over the aperture plane. The right hand column shows the displacements: in the aperture plane, parallel to the elevation axis, in the aperture plane normal to the elevation axis, and normal to the aperture plane.

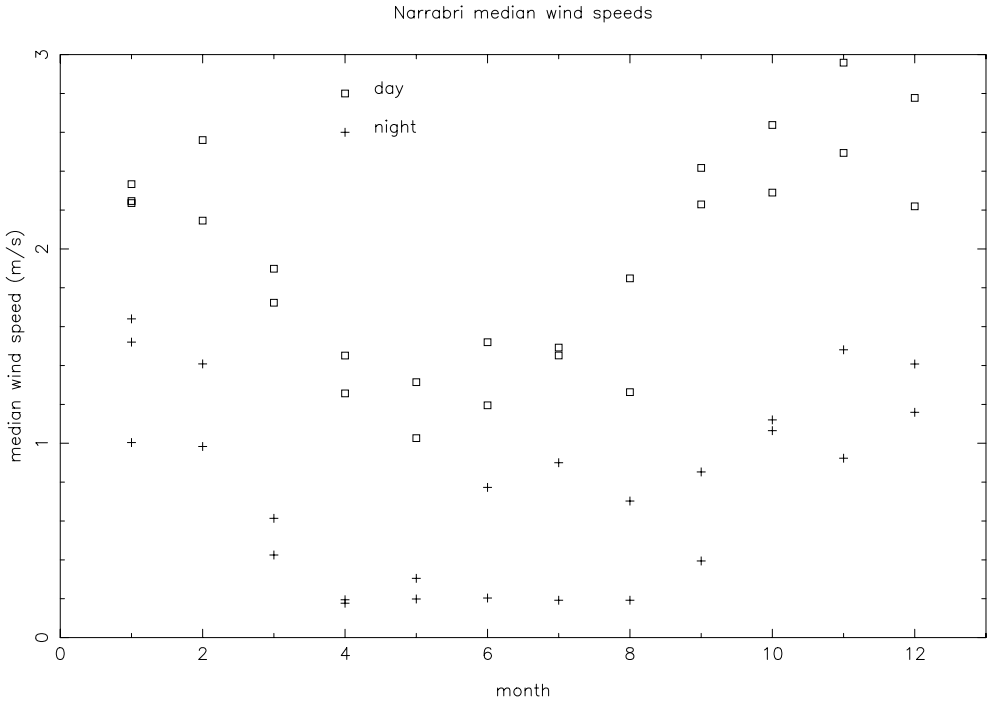

Figure 2: The median wind wind at Narrabri observed over the past two years.

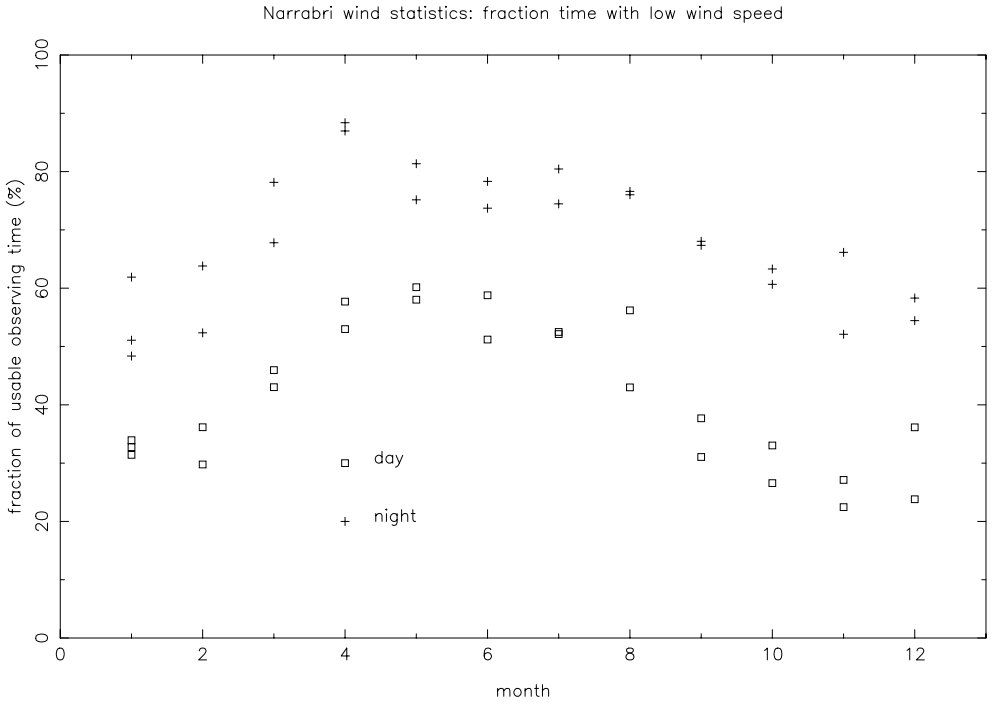

Figure 3: The fraction of time with wind speeds below the critical speed at which the wind-induced pointing error reaches one arc-second (at the worst orientation)

3 Servo Loop Issues

The ACC uses a PID servo loop with velocity feed-forward:

$$\text{requested rate} = \text{target velocity} + \text{GAIN} * (\text{err} + \text{C} * \int \text{err})$$

This is a robust algorithm which has served us well; alternative algorithms such as the H_∞ controllers (Gawronski, 1996, Kennedy, 1985) are recommended in conditions where tight control in the presence of random wind gusts is required.

The current pointing stability experiments should be expanded to include a detailed monitoring of the ACC servo loop.

4 Thermal Deformations

Thermal deformation of the pedestal and alidade structures are likely to have a long time-scale, given the extensive thermal insulation applied to the critical elements. The reference pointing histories do provide an indication that this is the case: there is now little evidence of a strong diurnal cycle. (The 1.5 "/C tilts have largely gone now that the fans in the ducts have been stopped).

Deformations in the backup structure are hard to quantify. At night, in still air we might expect a change in focal length if the steel immediately below the surface were to be offset by a few degrees from the rest of the backup structure - 2 degrees would result in ΔF $\sim$ 0.5 mm.

5 Current Pointing Accuracy

5.1 pointing stability

The Narrabri system has an on-line facility for determining the pointing errors. It is invoked after a reconfiguration in order to determine the pointing model; it is also invoked in reference pointing mode to determine the local pointing corrections. (McKay, 1997). An experiment was run in early February (Feb 9, from UT 4hrs to UT 12 hrs) in order to assess the limitations and capabilities of this machinery.

We distinguish several different types of error:

(a). The short term error (the 5-10 second error). This is in effect equivalent to a measurement error; it will be affected by the NPL encoder errors; the response of the servo control loop; and the signal-to-noise of the target source. Wind gusts could also be a factor.

(b). The long term error. This will be driven by the quality of the pointing model; by changes in the antenna environment - temperature and wind. The reference pointing technique is intended to mitigate these factors.

Embedded in a long experiment were a number of reference pointing checks. Each check consisted of three separate pointing determinations; the scatter in the results within each triplet measures the short-term error. The scatter between triplets measures the long-term error. The results are summarised in Table 3. The measurements were made in continuum mode, at 8.640 GHz, on strong pointing calibrators (S $\sim$ 2.5 Jy). The weather conditions were calm, with wind velocities typical for this time of year (see figure 6 and figure 7).

Table 3: The accuracy of the pointing determinations

	σ (az) (arcsecs)	σ (el) (arcsecs)
short-term (average over all antennas)	2.0	2.5
long-term (reference pointing mode)	2.4	2.5
long-term (blind pointing)	7	7

The long-term error (reference pointing mode) needs some explanation: at roughly one-hour intervals a triplet of source position measurements was made; the pointing model was then updated so that the source was on boresight. The observer's pointing error therefore varies from essentially zero immediately after the pointing update to the measured error at the time of the next update.

Let σ_m be the measurement rms (the short term error). Let σ_r be the rms of the differences in the successive reference pointing measurements. Let σ_o be the pointing rms that the observer encounters in the reference pointing mode. The antenna's long term contribution is harder to describe. It is likely to be quite slowly varying - due, for example, to the diurnal temperature cycle. As a first pass, I'll assume that it varies linearly with time between reference pointing updates. Define σ_a to be the rms in the true pointing change that occurs between reference pointing updates - it would be equal to σ_r if the measurement error were zero.

$$\sigma_r^2 = \sigma_m^2 + \sigma_a^2 + \sigma_m^2$$

The first term on the right arises because the reference pointing correction is corrupted by the measurement error.

The second term is the change that occurs between updates.

The third term is the measurement error in the second reference pointing.

The observer's rms is given by:

$$\sigma_o^2 = \sigma_m^2 + \frac{\sigma_a^2}{3}$$

The second term on the right results from the assumption of a linear change between updates.

The results in Table 3 are an average over time (the time between pointing updates) and over the 6 antennas.

5.2 tracking stability

In a second experiment strong pointing calibrators were tracked for long periods with the antenna pointing offset by one half-beamwidth from the source. Figure 4 shows the data for antennas 1 to 5 while pointing at the azimuth half-power point. The important point to note is that all four IFs (XX/YY at 8640 and XX/YY at 8768 MHz) are highly correlated within an antenna, and not correlated from one antenna to the next. Figure 5 shows the calibration scans, with all antennas on boresight. Table 4 summarises the results for all antennas, all offsets. A linear trend was removed from each track; this was necessary because an ideosyncrasy in the control system precluded true

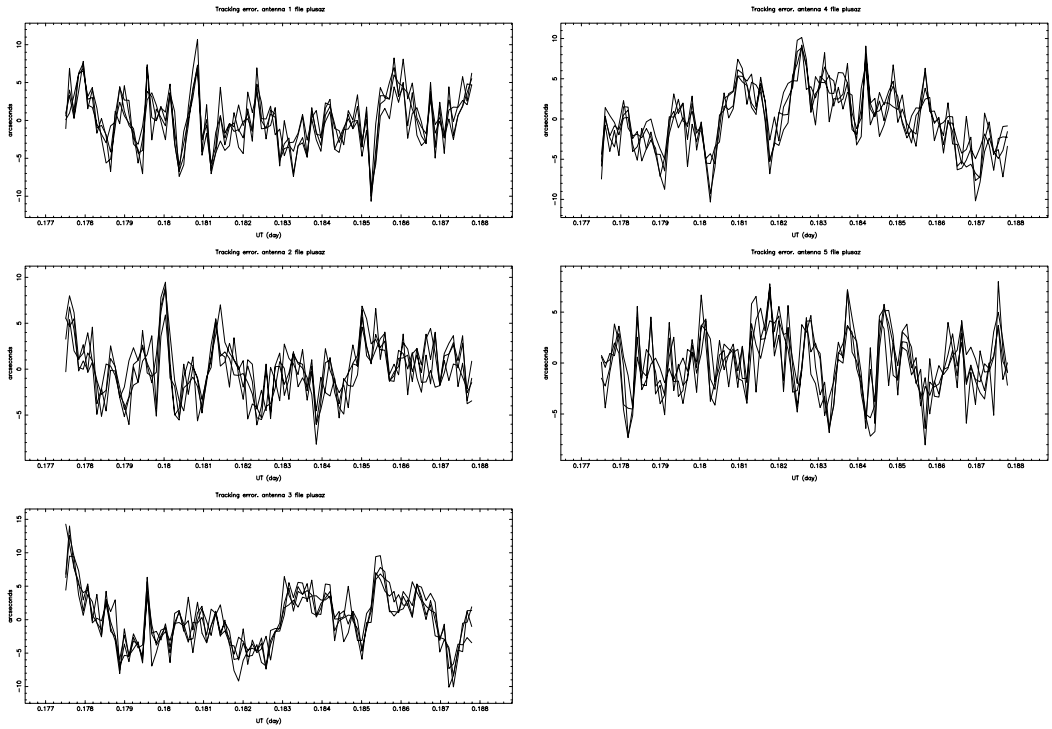

Figure 4: Tracking Error - azimuth offset

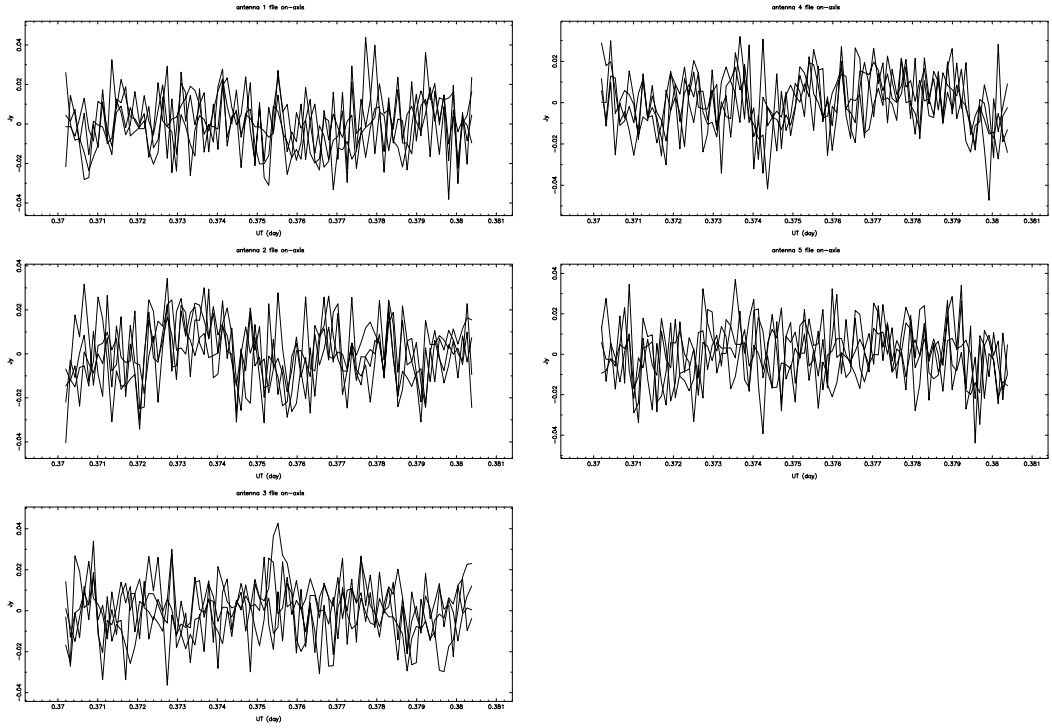

Figure 5: Reference stability - boresight observation

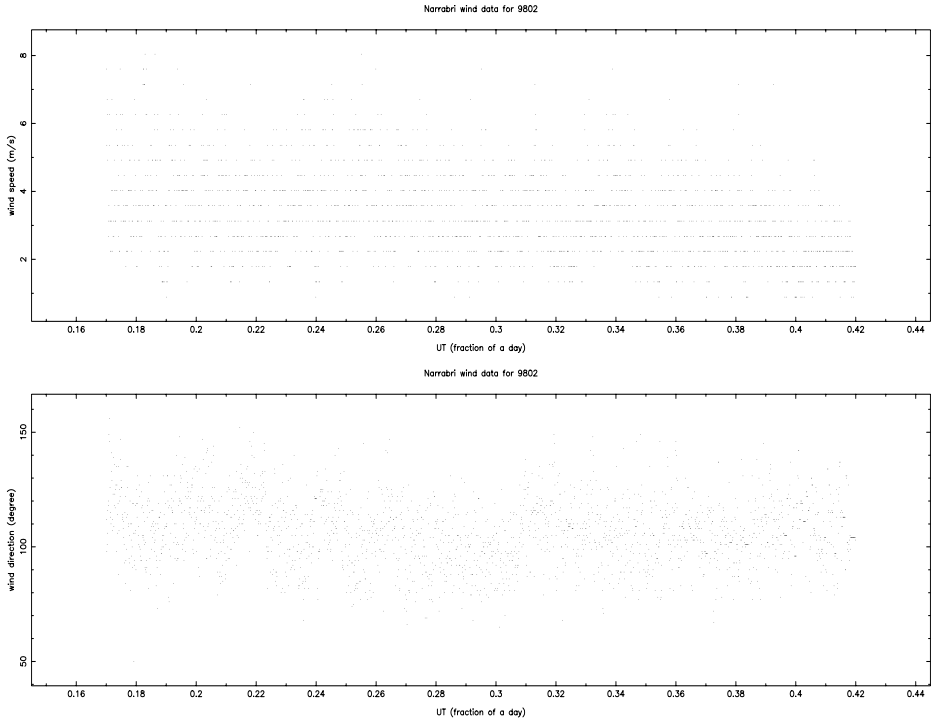

Figure 6: The Narrabri wind data for February 9, 1998

azimuth offsets; it also corrected for any slow antenna deformations. Figure 6 shows the detailed wind data for the observing period.

5.3 discussion

Both experiments indicate that the short-term rms is around 2 arcsecs on each axis. But signal-to-noise considerations indicate that we should be able to achieve better results (see, eg, MMA memo 189). With 6 antennas, system temperatures of 40 K, and 10 second integrations, the rms should be below 1 arcsec. Some possibilities :

(a). The NPL encoders' specifications quote 3.6 arcsec (peak).

(b). The median wind speed for much of this experiment was around 3 m/s. At this speed the wind loading calculations, at the most unfavourable wind/antenna orientation, indicate an error of 4 arcsecs.

(c). A significant improvement in the tracking stability occurred when I switched sources - from 1934-638 at az/el (205,25) to 0438-436 at (130,66).

Table 5 summarises the wind-antenna geometry effects present in the tracking experiment. The angle θ gives a measure of the probable wind deformation; a large angle (for a given wind speed) results in the largest pointing error. ζ shows how the error is distributed between azimuth and elevation. The abrupt decrease in the tracking error occurred when the elevation changed, and seems unrelated to the wind-antenna geometry. This suggests that the tracking error is set by the atmosphere, consistent with M. Holdaway's anomalous refraction argument.

(tentative) conclusion #3

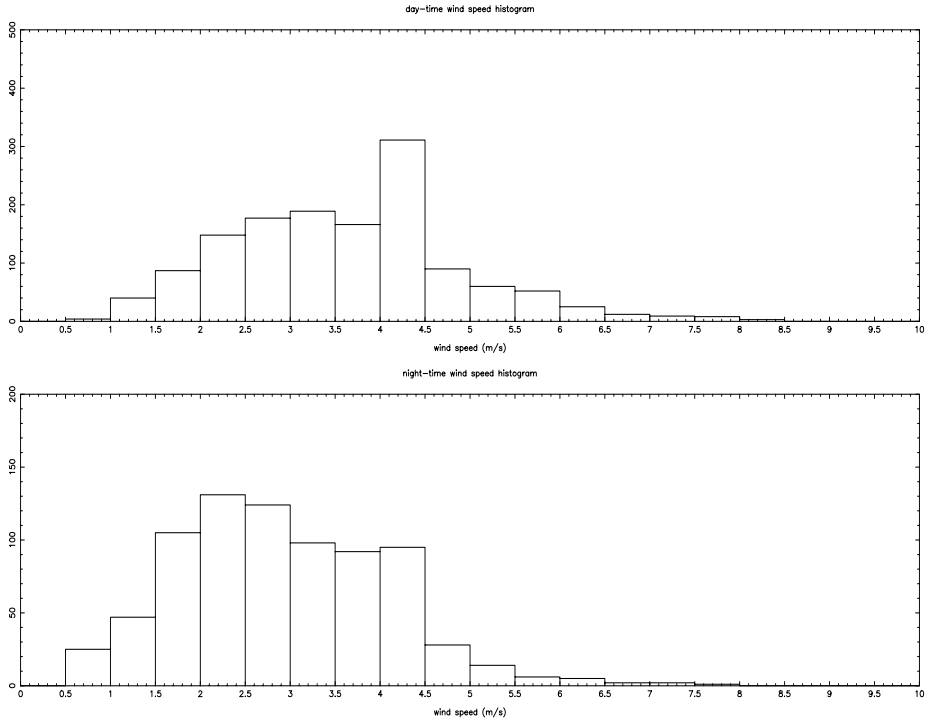

Figure 7: The Narrabri wind data in histogram form, split into daytime and nighttime plots

We might anticipate tracking errors of 1.5 arcsec/axis at night, during the mm season, at elevations above 40 degrees.

conclusion #4

A reference pointing frequency of around once/hour seems advisable to keep the pointing error below 2 arcsec/axis.

conclusion #5

More tracking experiments in different wind conditions are required.

6 Anomalous (and nomalous) refraction

The term "anomalous refraction" was coined by Altenhoff et al (A & A, vol. 184, 1987). Large pointing anomalies of up to 10-20 arcsecs have been observed at Pico Veleta and at Effelsberg. The effect has been discussed in more detail by Downes and Altenhoff (URSI/IAU symposium on RadioAstronomical Seeing, 1989) and also by Church and Hills (URSI/IAU symposium). The serious anomalies at the JCMT and at Pico Veleta are thought to be associated with an inversion layer rising to the altitude of the observatory - this is probably not an issue for Narrabri. The effect should be detectable in the interferometer phases.

Holdaway and others (MMA #186, 188) have used the term to describe the pointing fluctuations to be expected under normal conditions - in effect the bulk of the radio seeing. His expression for the pointing jitter is :

Table 4: The Antenna Tracking Stability expressed as a pointing rms (asecs)

offset	azimuth	elevation	CA01	CA02	CA03	CA04	CA05
az+	209	40	3.0	2.3	3.4	3.5	2.2
az-	210	38	3.4	3.6	3.2	2.4	3.5
az+	210	36	2.8	3.5	3.8	2.7	3.9
el+	211	35	2.8	3.1	1.9	2.4	3.1
el-	211	33	3.0	1.7	2.1	2.8	3.5
az-	210	30	3.2	2.5	3.1	2.5	2.6
az+	210	28	2.5	3.1	3.1	3.6	2.9
el+	210	27	2.8	3.3	2.7	2.8	4.5
el-	209	25	3.8	3.7	4.5	4.3	5.1
az-	130	66	1.5	1.4	1.4	1.6	1.0
az+	133	68	1.2	1.2	1.5	1.5	1.3
el+	138	71	2.1	2.3	2.0	2.0	2.6
el-	143	72	1.8	2.1	1.7	1.8	2.3
az-	167	76	1.1	1.3	1.3	1.5	1.5
az+	178	77	1.3	1.5	1.4	1.8	1.7
el+	191	76	1.5	1.7	1.3	2.1	2.9
el-	201	76	2.0	1.6	1.1	1.8	2.5

$$\sigma_p(d,z) = \frac{\sqrt{2D_l(d)\sec(z)}}{d}$$

for an antenna of diameter d, at a zenith angle z. $\sqrt{D_l}$ is the "root phase structure" function. (Since the precise details of this calculation are still under debate - witness the 3 MMA memos on the issue - a detailed quantitative match should not be expected yet; but the results are probably good to a factor of two or so).

The Narrabri structure function, obtained by R. Sault after detailed studies of the DQO observations, averages to :

$$D_l(d) = k * (d/1\ km)^{\beta}$$

with k $\sim$ 1, and $\beta \sim 0.8$. This leads to a pointing rms of :

$$\sigma_p = 2.9\sqrt{\sec(z)} \text{ arcsecs}$$

This is a bit larger than we observed, but not greatly. The elevation angle dependance is fine.

7 Conclusions

1. The strict mosaicing requirements ($\sigma < 1.5$ arcsecs) are difficult to meet.
2. The atmosphere may the limiting factor.

Table 5: The wind-antenna geometry effects

wind speed		wind dirn		track err	antenna		wind-antenna angles	
mean	rms	mean	rms		az	el	θ	ζ
(m/s)		(degrees)		(asec)			(degrees)	
3.90	1.35	111.9	15.3	2.9	209	40	95	81
3.71	1.44	110.1	14.7	3.2	210	38	98	77
3.64	1.20	114.6	14.6	3.4	210	36	94	84
3.49	1.20	112.5	13.7	2.7	211	35	97	79
3.35	1.09	113.4	15.5	2.7	211	33	97	79
3.66	1.42	113.4	11.8	2.8	210	30	96	81
4.07	1.35	99.5	14.1	3.1	210	28	108	63
3.66	1.23	108.9	13.2	3.3	210	27	100	75
3.65	1.14	98.1	15.0	4.3	210	25	109	61
2.74	0.99	109.8	14.3	1.4	130	66	68	18
3.41	1.04	107.0	14.3	1.3	133	68	70	24
3.79	1.22	104.5	13.7	2.2	138	71	74	32
2.77	0.96	104.7	15.2	1.9	143	72	76	37
2.87	1.15	102.3	10.5	1.3	167	76	84	64
2.94	0.97	108.9	13.4	1.6	178	77	85	68
2.23	1.00	112.2	12.2	2.0	191	76	87	79
2.30	0.68	107.5	14.1	1.9	201	76	91	87

θ is the angle between the wind vector and the radio axis.
ζ is the position angle of the wind-induced pointing error.

8 References

Altenhoff, W.J., Baars, J.W.M., Downes, D., Wink, J.E., Astron. and Astrophys, **184**, 381 (1987).

Butler, B. MMA Memo **188** (1997)

Church, S. and Hills, R. URSI/IAU symposium on RadioAstronomical Seeing, Beijing, (1989). Ed : Baldwin and Shouguan. p. 31

Downes, D. and Altenhoff, W.J. URSI/IAU symposium on RadioAstronomical Seeing, Beijing, (1989). Ed : Baldwin and Shouguan. p. 75

Fox, N.L. Load Distributions on the surface of Paraboloidal Reflector Antennas. JPL Internal Memorandum **CP-4** (1962).

Gawronski, W. TDA Progress Report **42-127**, (Nov. 1996)

Holdaway, M.A. MMA Memo **178**. (1997)

Holdaway, M.A. MMA Memo **186** (1997).

Kennedy, R.A. Digital Servo Control of a Large Radio Telescope. M.E. thesis presented to University of Newcastle (1985).

Lucas, R. MMA **189** (1997).

McKay, D. M.Sc thesis presented to UNSW (1997). Also the on-line documentation at Narrabri.

Melbourne, W.H. and Cheung, C.K. Wind Tunnel Measurements on a Model of the Antenna Element

of the Australia Telescope (1983). AT document AT/12.5.3.4/008

file : /epp/source1/mjk/mnrf/txt/pointing.tex